

Interactive Chan-Vese Approach with Random Walk for Medical Images Segmentation

Mohammadreza Hosseini¹, Arcot Sowmya¹ and Tomasz Bednarz²
¹*School of Computer Science and Engineering, UNSW, Kensington, Sydney, Australia*
²*Science and Engineering Faculty, QUT, George St, Brisbane, Australia*

Keywords: Interactive, Chan-Vese, Random Walk, Energy Function.

Abstract: In this paper, we present a novel interactive variational approach to image segmentation within a Chan-Vese framework. We propose a parameterized energy function that can be modified based on user input, and also incorporate in it a probabilistic term that defines reachability of a pixel from a user-selected 'internal' object pixel. The proposed approach shows promising improvement over automatic segmentation methods when applied to medical images.

1 INTRODUCTION

Segmentation involves separating an image into regions with some similarities. Segmentation by evolving a contour to detect an object boundary has been discussed before (Chan and Vese, 2001), (Kass et al., 1988). Object detection is achieved by minimizing the energy associated with the current contour, usually modeled as the sum of an internal and external energy. Level set methods are another approach to detect object boundaries in an image (Malladi et al., 1995). The central idea is to represent an evolving contour using a signed distance function, where its zero level is correlated to the actual contour. Then, according to the motion equation of the contour, a similar flow for the implicit surface can be estimated. The optimal surface zero level set is then used to determine the object boundary. The surface flow when applied to the zero level will reflect the propagation of the contour. External energies relying on the image gradient alone can miss object borders that are not necessarily defined by their gradient. The Chan-Vese level set method uses a stopping term instead, that relies on the similarity of intensities in the object against the background (Chan and Vese, 2001). The basic assumption in the Chan-Vese method is that two regions of approximately piecewise-constant intensity form the image. In images where this assumption is violated because of the presence of different objects with different intensities, Chan-Vese fails to segment the objects

from the background. This is the main reason that experienced observer inputs continue to be important for image data segmentation, especially medical images (Ben-Zadok et al., 2009). In this paper, an interactive Chan-Vese method with user inputs, provided as a series of selected pixels inside the object of interest, will be explored. The segmentation effects of adding another energy term that models the probability of getting from a pixel to one of selected pixels inside the object, will also be studied.

The outline of this paper is as follows. In the next section, a brief overview of the interactive segmentation approaches is provided. A brief overview of active contours is provided in section 2.1, followed by a full description of the Chan-Vese method in section 2.2. In section 3 we introduce a novel energy minimization model and discuss its relationship to the Chan-Vese segmentation approach. In section 3.1 a reachability term that increases segmentation accuracy is added to the proposed energy function. In section 4, we validate our model by performing experiments on real medical images, showing the advantages of the proposed method, and we end the paper with a brief concluding section.

2 BACKGROUND

To overcome the limitations of automatic segmentation methods, researchers have proposed

new human collaborative techniques that guide the segmentation towards the object of interest (Zhao et al., 2013). This collaboration mostly occurs by means of the user providing an object shape prior, selecting some seeds inside the object of interest, or providing boundaries around the object of interest. The forms of collaboration differ mainly by the type of human interaction. Prior information about object shape or intensity distribution can be used in the energy function and the posterior distribution computed from the prior. Energy minimization usually leads to selecting a segmentation that has higher posterior. These approaches are usually referred to as Bayesian methods for image segmentation (Cremers et al., 2007; (Cremers et al., 2007).

In images where objects and background may exhibit very similar intensity characteristics, higher-level prior knowledge about the shape of an expected object can be merged in the Bayesian formulation of the image segmentation problem (Tsai et al., 2003). The use of graph-edge weights that contain information about a level-set function of a template, in addition to the usual boundary and region terms, is another Bayesian approach for image segmentation using prior shape (Chang et al., 2008). This allows the edges of the graph to convey information about the image as well as the prior shape knowledge.

Boykov and Jolly (2001) and Boykov and Kolmogorov (2000) proposed a very effective graph cut approach for interactive image segmentation. An initial trimap $T = \{T_F, T_B, T_U\}$ partitions the image into three sets: T_F is the set of foreground pixels selected by the user, T_B the set of background pixels also selected by the user, and T_U the set of unmarked pixels. It is assumed that the intensity distributions of the foreground and background are either known prior, or assembled directly from labeled pixels in the respective trimap. For every pixel, an energy function that evaluates the fit of the pixel to the data model is computed. This energy function encourages coherence in regions of similar intensities. The graph cut algorithm adjusts the current segmentation efficiently without recomputing the whole solution from scratch when new seeds are incorporated into the system. GrabCut (Kolmogorov and Blake, 2004) is the first modification of the basic graph cut segmentation model. In this approach the user defines a bounding box around the object to be segmented. The intensity distributions of the target object and the background are estimated using a Gaussian mixture model. This is used to construct a Markov random field over the pixel labels, with an

energy function having internal energy that prefers connected regions to have the same label. Using a graph cut approach to minimize the function, the pixel labels are estimated. This estimate is expected to be more accurate than the original, and the two-step procedure is repeated until convergence. The absence of strong boundaries and the presence of a number of objects with similar intensity profile in some medical images cause this method to fail. Incorporation of shape priors using a level-set template within this framework may minimize these problems (Freedman and Zhang, 2005).

Another type of interactive segmentation method works by selecting seeds inside the object of interest, with no prior information about the foreground and background assumed (Ben-Zadok et al., 2009). Based on user selected seeds, a new energy term is incorporated in the energy function. This energy term prefers that selected seeds are part of the final object segmentation. Another approach to interactive segmentation is through belief propagation (Zhu et al., 2010), which starts with the user selecting seeds inside the object of interest. The method iteratively estimates the belief of one labeled pixel about other pixels having the same label. Belief integration is then used to compute the pixel label.

Random walk performs multi-label, interactive image segmentation (Grady, 2006; Kumar et al., 2013). Given a small number of pixels with user-defined labels, the algorithm starts by determining the probability that a random walker starting at each unlabeled pixel will reach one of the pre-labeled pixels. By assigning each unlabeled pixel to the label that has the greatest probability, high-quality image segmentation is obtained.

To improve the efficiency of this approach the use of image priors to find disconnected pieces of an object was proposed (Ruiz et al., 2015); (Grady 2005), while removing the necessity of user interaction.

Interactive segmentation in all of the above-discussed methods is implemented by aggregating user input in an energy function. It is reasonable to ask how the methods will perform if instead of extracting a single feature based on user input, multiple features were extracted and integrated with the energy function. As will be discussed in this paper, creating more features from user input and defining energy functions based on these new features, improves the accuracy of the interactive method. This improvement is especially significant in decreasing the number of pixels that are incorrectly classified as an object.

2.1 Active Contour

The active contour model or “snakes” is a framework for extracting objects from possibly noisy 2D images (Kass et al., 1988). This framework attempts to minimize the energy associated with the current contour as a sum of an internal and external energy such that:

- i. The external energy is minimal when the snake is at the object boundary position
- ii. The internal energy is minimal when the contour has a shape that is ‘similar’ or ‘close’ to the shape of the sought object.

In order to guarantee the stability of contour evolution, mechanisms are used to avoid overlap of control points, which also enables the splitting and remerging of contours during evolution (Osher et al. 1988). Two general issues with snakes, including poor convergence of concave boundaries and low performance of poor initialization, can be solved using a gradient vector flow (GVF) snake model (Xu et al. 1988). This new active contour external energy is computed as spatial diffusion of the gradient of an edge map extracted from the image. For overcoming the high computational time of GVF, other approaches such as speedup GVF that require less time to estimate the diffusion process is also proposed.

2.2 Chan-Vese Approach

The Chan-Vese method (Chan and Vese 2001) provides a model for detecting objects in an image using the active contour and Mumford Shah’s model, when boundaries are not defined by gradients.

Let $I: \Omega \rightarrow \mathbb{R}$ where $\Omega \subset \mathbb{R}^2$ be an image. Let $X = (x, y)$ specify the coordinates of the pixels in the image I . It is assumed that the image is composed of two objects (background and foreground). The goal is to evolve a curve C , such that C is at the boundary of the object in the image. Defining c_1, c_2 as the average intensities of pixels inside and outside of the curve respectively, the Chan-Vese method defines the energy function $F_\varepsilon(c_1, c_2, C)$ as follows:

$$\begin{aligned} F_\varepsilon(c_1, c_2, \phi) = & \mu \int_{\Omega} \delta_\varepsilon(\phi(x, y)) |\nabla \phi(x, y)| dx dy \\ & + \vartheta \int_{\Omega} H_\varepsilon(\phi(x, y)) dx dy \\ & + \lambda_1 \int_{\Omega} |I(x, y) - c_1|^2 H_\varepsilon(\phi(x, y)) dx dy \\ & + \lambda_2 \int_{\Omega} |I(x, y) - c_2|^2 (1 - H_\varepsilon(\phi(x, y))) dx dy \end{aligned} \quad (1)$$

where $\mu \geq 0, \vartheta \geq 0, \lambda_1, \lambda_2 > 0$ are fixed parameters, H is a Heaviside function and $C \subset \Omega$ is represented by the zero level set of function $\phi: \Omega \rightarrow \mathbb{R}$ such that

$$\begin{cases} C = \{(x, y) \in \Omega: \phi(x, y) = 0\} \\ \text{inside}(C) = \{(x, y) \in \Omega: \phi(x, y) > 0\} \\ \text{outside}(C) = \{(x, y) \in \Omega: \phi(x, y) < 0\} \end{cases} \quad (2)$$

3 INTERACTIVE CHAN-VESE METHOD

Assume that user inputs $\{X_i = (x_i, y_i) | i = 1 \dots N\}$ are available. These points are selected by the user and are inside the object of interest, which we will refer to as seeds. The assumption is that the intensities of the selected seeds are a good representation of the pixel intensities inside the object. We define

$$\begin{aligned} lT &= \min\{I(X_i) | i = 1, \dots, N\} \\ uT &= \max\{I(X_i) | i = 1, \dots, N\} \end{aligned} \quad (3)$$

which are the maximum and minimum of seed intensities. We design two new energy terms where one is penalized if the segmentation includes objects with intensities lower than lT or higher than uT , and the other one is penalized if the segmentation does not contain objects with intensities in the range $[lT, uT]$. The two functions L_1 and L_2 are defined as follows:

$$\begin{aligned} L_1(X) &= \left(\frac{2X - lT}{uT - lT} - 1 \right)^{k_1} \\ L_2(X) &= e^{-\left(\frac{2X - (uT + lT)}{uT - lT} \right)^{k_2}} \end{aligned} \quad (4)$$

where k_1, k_2 are positive even integers. To incorporate user feedback in the formulation of the energy term in the original Chan-Vese model, we introduce L_1 and L_2 into the original formulation as follows:

$$\begin{aligned} F_{user}(\phi) = & \mu \int_{\Omega} \delta_\varepsilon(\phi(x, y)) |\nabla \phi(x, y)| dx dy \\ & + \vartheta \int_{\Omega} H_\varepsilon(\phi(x, y)) dx dy \\ & + \lambda_1 \int_{\Omega} L_1(I(x, y)) H_\varepsilon(\phi(x, y)) dx dy \\ & + \lambda_2 \int_{\Omega} L_2(I(x, y)) (1 - H_\varepsilon(\phi(x, y))) dx dy \end{aligned} \quad (5)$$

Clearly, $F_{user}(\phi)$ will be minimized if pixels with intensities in the range $[lT, uT]$ are within the segmented region, and pixels with intensities outside the range are outside the segmented region. The results of applying this new energy function within the Chan-Vese framework on various biomedical images are displayed in Fig 1. It is obvious that for

some segmentation problems, the method performs well, but in other cases, where there are many objects in the same intensity range as the object of interest, the segmentation may not be aligned with user expectation. To overcome these limitations, an additional energy term is introduced into the definition of the energy function. This new term will be referred to as reachability and is discussed next.

3.1 Reachability

To improve the generalizability of the proposed method, a reachability concept is utilized to guide the flow of the level set function. Reachability $\mathfrak{R}(x, y)$ is defined as the probability of getting from a pixel (x, y) to one of user-selected seed pixels by moving randomly inside the image. It is assumed that each pixel is connected to its four neighbours and every edge connecting a pixel to its neighbour has a weight. An edge with larger weight has a higher chance of being picked for the next movement from the current pixel. It can be argued that by adding a reachability component to the energy function developed in the last section, the user can more specifically select an object from an image. In the new energy function, seeds are not only used to select the intensity range, but also to remove other objects, which are not reachable from the seed pixels. Reachability is inspired by random walk based segmentation (Grady 2006). It is assumed that the image is represented as an undirected weighted graph $G = (V, E)$ where V is the set of image pixels and E is the set of pairs of four neighbour pixels in the image. These graph weights are defined in such way that similar pixels have weights with higher values. In our approach similar pixels are those whose intensities are in the range of $[lT, uT]$. Based on this assumption, a new weight function is developed that assigns higher weights to edges with both vertices in the required range. For every $v_i, v_j \in V$ where $(v_i, v_j) \in E$, the edge weight is defined as

$$w(v_i, v_j) = e^{-\frac{d(v_i, v_j)}{\sigma^2}} \quad (6)$$

Where

$$d(v_i, v_j) = \left(\left(I(v_i) - \frac{(lT+uT)}{2} \right)^2 + \left(I(v_j) - \frac{(lT+uT)}{2} \right)^2 \right) \quad (7)$$

and $I(v)$ is the image intensity at v . In (7), edges with end pixel intensities very close to the centre of the range have the lower value of $d(v_i, v_j)$ and as a result have a higher weight compared to other edges.

To calculate reachability \mathfrak{R} , the set V of image pixels is partitioned into three different sets: “labeled set” V_m , which are the seeds, “labeled background” V_b , which are pixels that definitely are not part of the object since their intensities are not in the range $[lT, uT]$, and “Unlabeled set” V_u , which are the remaining pixels. It turns out that $\mathfrak{R}(x, y)$ is the harmonic solution to a combinatorial Dirichlet problem with the seed labels as the boundary condition (Grady 2006). The harmonic function that satisfies the boundary condition also minimizes the Dirichlet integral $D(x)$. By defining the combinatorial Laplacian matrix as

$$L_{ij} = \begin{cases} \partial_i & \text{if } i = j \\ -w_{ij} & \text{if } i \text{ and } j \text{ are adjacent} \\ 0 & \text{otherwise} \end{cases} \quad (8)$$

and assuming that the nodes in L are ordered such that seed nodes are first, background nodes are second and unseeded nodes are third, $D[x]$ can be decomposed as

$$D[x_u] = \frac{1}{2} [x_m^T, x_b^T, x_u^T] \begin{bmatrix} L_m & C & B \\ C^T & L_b & A \\ B^T & A^T & L_u \end{bmatrix} \begin{bmatrix} x_m \\ x_b \\ x_u \end{bmatrix} \quad (9)$$

where $x_m(x, y)$, $x_b(x, y)$ and $x_u(x, y)$ correspond to the reachability of the seeded, background and unseeded nodes respectively. Differentiating $D[x_u]$ with respect to x_u and finding the critical points yields

$$L_u x_u = -B^T x_m \quad (10)$$

where x_u is the reachability of unseeded pixels. Since the reachability of the seeded pixels is one and background pixels have zero chance of reaching the seeded pixels, $\mathfrak{R}(x, y)$ can be expressed as:

$$\mathfrak{R}(x, y) = \begin{cases} 1, & (x, y) \in V_m \\ 0, & (x, y) \in V_b \\ x_u(x, y), & (x, y) \in V_u \end{cases} \quad (11)$$

The proposed energy function is a modification of equation (5) and now can be defined as follows:

$$F = F_{user}(\phi) - \lambda_3 \int_{\Omega} \Gamma(\mathfrak{R}(x, y)) H_{\epsilon}(\phi(x, y)) dx dy \quad (12)$$

where F_{user} is the same as discussed in (5), $\lambda_3 > 0$ is a fixed parameter and $\Gamma(X)$, referred to as the gamma function, is selected in such a way that it has lower value for high reachability, and higher value for lower reachability. In the new energy function, every pixel is not only tested for its similarity with the intensity range of the object, but it is also evaluated for its reachability to one of the seeds. If

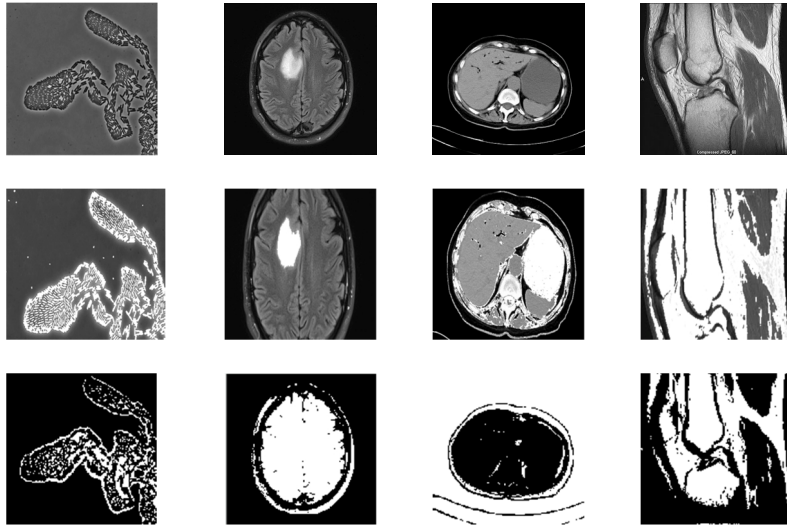


Figure 1: Applying the interactive Chan-Vese method on gray scale images. The first row shows the original images, second row shows the results of the interactive segmentation method in (5) and the third row the original Chan-Vese method. The first column is an image of a biofilm. The interactive approach can successfully detect the biofilm boundary. In the second column, the method can identify the boundary of the tumour. This is because the tumour has intensity range entirely different from other parts of the image. In the last two columns, the objects of interest are the stomach and Femur respectively; as there are other objects with the same intensity as the object of interest, some other pixels are also returned as the object, which is not the expected result.

the intensity of a pixel matches with the intensity range but it is not reachable, it will eventually be removed from the final segmentation.

$$TPP = \frac{TP}{TP + FN} * 100 \quad (13)$$

and the false positive percentage as:

$$FPP = \frac{FP}{TN + FP} * 100 \quad (14)$$

4 EXPERIMENTAL RESULTS

The performance of the proposed algorithm, which we shall refer to as “*Interactive Segmentation with Random walk*”, is tested experimentally. In Fig 2, the results of applying the interactive approach on a series of medical images are shown. It is obvious that the combination of intensity range and reachability in the definition of the energy function provides significant improvement, compared to each applied separately. To evaluate the accuracy of the proposed interactive method, extensive experiments were conducted on a series of lung images from 50 different patients.

For every patient, 5 slices of the 3D lung scans were selected and the boundaries were extracted by an experienced radiologist to produce the ground truth (Fig 3). The definitions used to compare the segmentation results to ground truth appear in Table 1. Based on these definitions, the true positive percentage is defined as :

The average and standard deviation of true positives and false positives computed over all patient images are shown in Figs 4 and 5, and establish that Interactive segmentation with random walk has nearly the same average true positive value as Chan-Vese, while providing a much better average false positive value.

The proposed algorithm was further evaluated on the test dataset using two other well-known interactive segmentation methods, namely random walker and (Grady 2006) and GrabCut (Kolmogorov and Blake 2004). As Figs 6 and 7 reveal, GrabCut has higher performance in detecting true pixels inside the object, but is worst among the three in removing unrelated pixels.

The bounding box around an object of interest can describe more comprehensively the object intensity variations compared to a few seeded pixels selected by the user. This could explain the higher true positive percentage of GrabCut in comparison to the other two methods. At the same time, the interactive segmentation with random walk approach performs better compared to random walker alone.

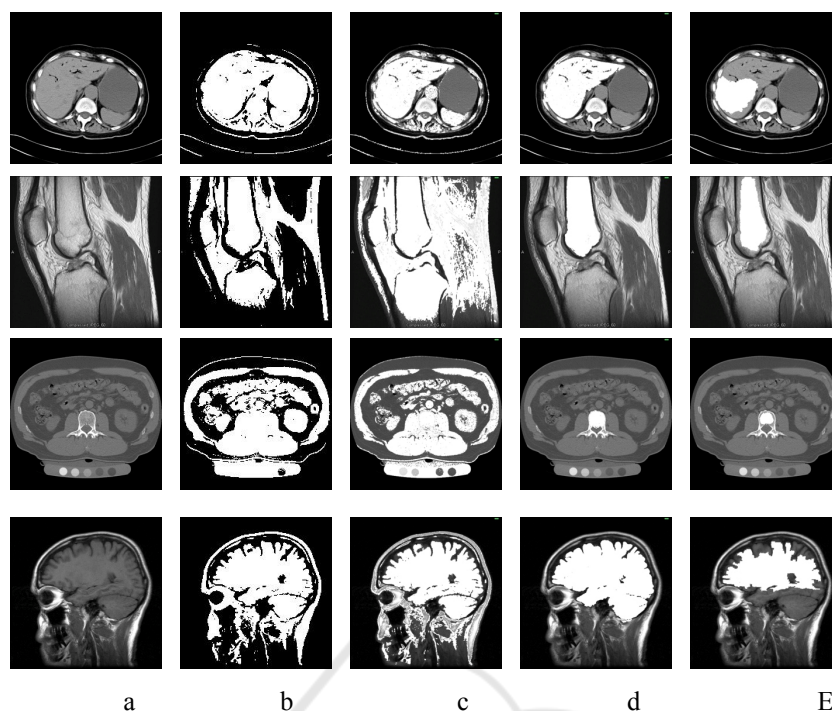


Figure 2: Results of applying different methods for extracting region of interest from an image a) Original images b) Automatic Chan-Vese method, no control over the region of interest c) Proposed method without reachability ($\lambda_3=0$) d) Proposed method with reachability ($\lambda_3 > 0$) e) Segmentation using only reachability in definition of energy function.

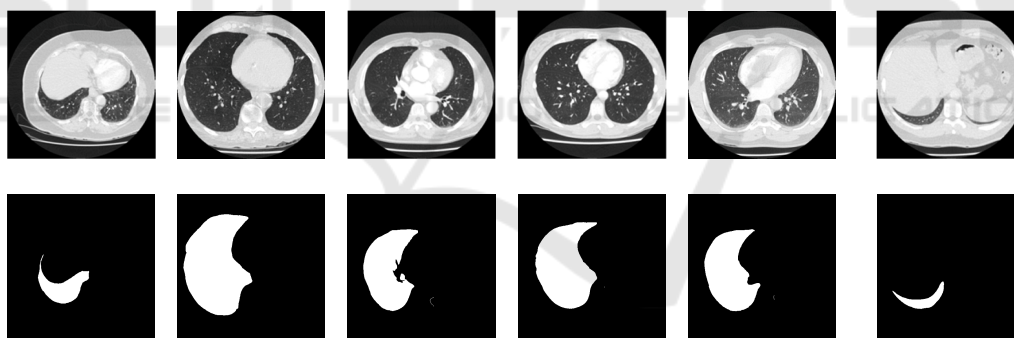


Figure 3: Lung image data set taken from 50 different patients. The first row is the original image and the second row is the right lung detected by an experienced radiologist.

Table 1: Metrics used for comparing the segmentation results.

	Detected as foreground	Detected as background
Foreground Pixel	True Positive (TP)	False negative (FN)
Background Pixel	False positive (FP)	True negative (TN)

The high FPP of GrabCut in comparison to the other two methods is because there is a chance that unrelated pixels inside the object of interest might also contribute to the object Gaussian mixture model, resulting in a higher FPP. As shown in these figures, the interactive segmentation with random walk approach has low average FPP, which means that it is able to remove unrelated pixels from the final segmentation. At the same time, it performs better than random walk in retaining related pixels in the final segmentation.

In Figs 8 and 9, Dice Similarity Coefficient (DSC) and the ratio of true positive rate over false positive rate for all four different methods shows the promising results for the proposed Interactive segmentation with random walk method.

5 CONCLUSION

In this paper we propose a new method for detecting objects of interest based an interactive Chan-Vese method. The algorithm starts with the user selecting some points inside an object. The intensities of selected points are used to guide the flow of a level set method. To further refine the results, a reachability term is used in the definition of the level set energy function. The results show the superiority of our approach compared to the normal Chan-Vese approach as well as random walk segmentation alone in detecting true object pixels. It also outperforms GrabCut in identifying background pixels.

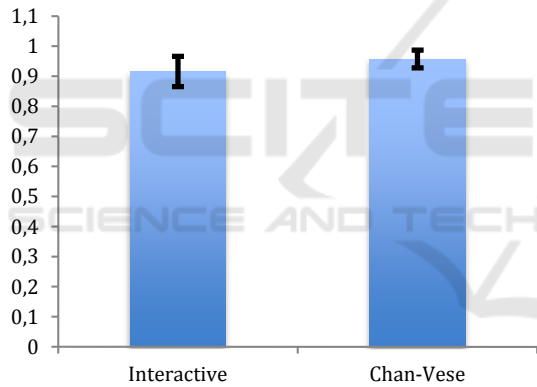


Figure 4: The average and standard deviation of true positives over all images.

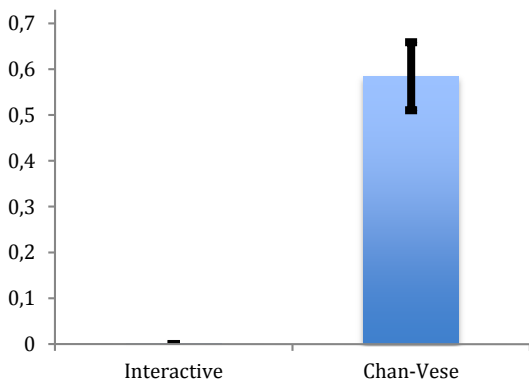


Figure 5: Average and standard deviation of false positives over all images.

In this work, we assume that the user selects pixels uniformly from a variety of intensities that may exist in the object of interest. The effect of non-uniform pixel selection inside the object of interest is worth further investigation.

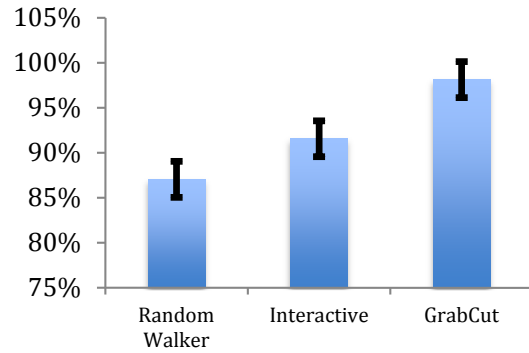


Figure 6: Average and standard deviation of TPP.

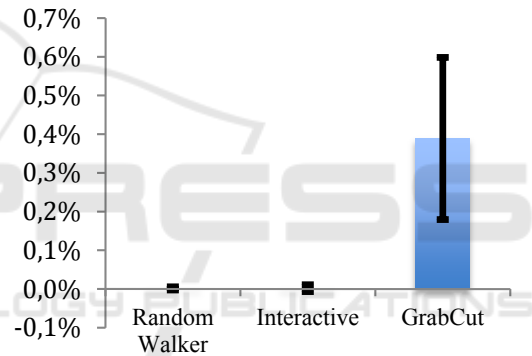


Figure 7: Average and standard deviation of FPP.

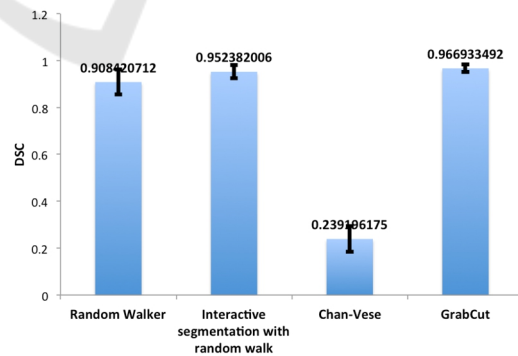


Figure 8: Dice Similarity Coefficient (DSC).

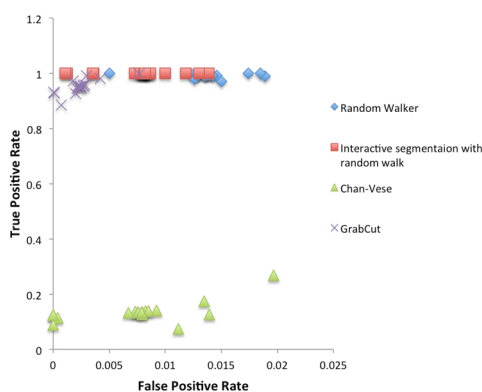


Figure 9: True positive rate vs. False positive rate.

REFERENCES

- Ben-Zadok, N., Riklin-Raviv, T., Kiryati, N., 2009. Interactive level set segmentation for image-guided therapy. In *IEEE Int. Symp. on Biomedical Imaging*, pages 1079-1082.
- Cremers, D., Fluck, O., Rousson, M., Aharon, S., 2007. A probabilistic level set formulation for interactive organ segmentation. In *Medical Imaging 2007: Image Processing*, 6512 (1): 120-129.
- Cremers, D., Fluck, O., Rousson, M., Aharon, S., 2007. A probabilistic level set formulation for interactive organ segmentation. In *Medical Imaging 2007: Image Processing*, 6512 (1): 120-129.
- Chan, T., Vese, L., 2001. Active contours without edges. In *IEEE Trans. Imag. Proc.*, vol. 10, pp. 266-277.
- Grady, L., 2006. Random walks for image segmentation. In *IEEE Trans. Pattern Analysis and Machine Intelligence*.
- Jha, S.K., Bannerjee, P., Banika, S., 2013. Random Walks based Image Segmentation Using Color Space Graphs. In *Procedia Technology*, Vol. 10, pp. 271-278.
- Boykov, Y., Jolly, P., 2001. Interactive Graph Cuts for Optimal Boundary & Region Segmentation of Objects in N-D Images. In *Proc. Int'l Conf. Computer Vision*, vol. 1, pp. 105-112.
- Rother, C., Kolmogorov, V., and Blake, A. 2004. Grabcut—interactive foreground extraction using iterated graph cuts. In *ACM Transactions on Graphics (SIGGRAPH)*.
- Freedman, D., Zhang, T., 2005. Interactive Graph Cut Based Segmentation with Shape Priors. In *Proc. IEEE Conf. Computer Vision and Pattern Recognition*.
- Malladi, R., Sethian, J.A., Vemuri, B.C., 1995. Shape modeling with front propagation: A level set approach. In *IEEE Trans. Pattern Anal. Machine Intell.*, vol. 17, pp.158-175.
- Kass, M., Witkin, A., Terzopoulos, D., 1988. Snakes: Active contour models. In *Int. J. Comput. Vis.*, vol. 1, pp.321-331 1988.
- Cremers, D., Rousson, M., Deriche R., 2007. A review of statistical approaches to level set segmentation: Integrating color, texture, motion, and shape. In *Int. J. Comput. Vis.*, vol. 72, no. 2, pp.195-215.
- Tsai, A., Yezzi, A., Wells, W., Tempany, C., Tucker, D., Fan, A., Grimson, E., Willsky, A., 2003. A shape based approach to curve evolution for segmentation of medical imagery. In *IEEE Trans. Medical Imaging*, 22(2).
- Chang, H., Yang, Q., Parvin, B., 2008. A Bayesian Approach for Image Segmentation with Shape Priors. In *IEEE Conference on Computer Vision and Pattern Recognition*.
- Boykov, Y., Kolmogorov, V., 2000. Interactive organ segmentation using graph cuts. In *Int. Conf. on Medical Image Computing and Computer-Assisted Intervention*, pages 276-286.
- Zhu, Y., Cheng, S., Goel, A., 2010. Interactive segmentation of medical images using belief propagation with level sets. In *Proc. 2010 IEEE Int. Conf. Image Process.*, pp.4113-4116.
- Ruiz, E., Kjer, H.M, Vera, S., Ceresa, M., Paulsen, P., González-Ballester, M.A., 2015. Random Walks with Shape Prior for Cochlea Segmentation. In *Proceedings of CARS 2015*.
- Grady, L., 2005. Multilabel random walker segmentation using prior models. In *IEEE Conference of Computer Vision and Pattern Recognition, San Diego, CA, June 2005*, vol. 1, pp. 763-770.
- Osher, S., Sethian, J.A., 1988. Fronts propagation with curvature-dependent speed: Algorithms based on Hamilton, Jacobi Formulation. In *Journal of Computational Physics*. 12-49.
- Xu, C., Prince, J.L., 1988. Snakes, shapes and gradient vector flow. In *IEEE image processing*. 359-369.
- Olszewska, J., De Vleeschouwer, C., Macq, B., 2007. Speedup gradient vector flow b-spline active contours for robust and real-time tracking. In *ICASSP*, 905-908.
- Zhao, F., Xie, X. 2013. An overview of Interactive Medical Image Segmentation. In *British Machine Vision Association and Society for Pattern Recognition*. 1-22.